Experimental $E(\vec{k})$ dispersions for the Zn 3d states: Evidence for itinerant character

F. J. Himpsel, D. E. Eastman, E. E. Koch,* and A. R. Williams
IBM Thomas J. Watson Research Center, P.O. Box 218, Yorktown Heights, New York 10598
(Received 2 June 1980)

Using angle-resolved photoemission from Zn (0001) we observe that the Zn 3d states exhibit energy-band dispersion (0.17 eV from Γ_6^+ to Γ_5^- for the upper d band) and k-dependent polarization selection rules. The d bands are centered at 10 eV below the Fermi energy E_F and are 1.0 eV wide (Γ_4^- to Γ_5^-). In contrast, *ab initio* band calculations using a Hedin-Lundqvist potential yield d bands centered at $\sim$8.3 eV below E_F that are 1.5 eV wide and disperse by 0.33 eV, thus indicating the significance of self-energy corrections for these deep-lying narrow bands. Upon empirically correcting the d-band position by adjusting the exchange parameter α in a nonrelativistic $X\alpha$ calculation, the calculated bandwidth (1.0 eV) and dispersion are also in agreement with experiment. Experimental critical points are (energies relative to E_F): $\Gamma_5^- = -9.60$ eV, $\Gamma_6^+ = -9.77$ eV, $\Gamma_6^- = -10.05$ eV, -10.30 eV, $\Gamma_5^+ = -10.05$ eV, -10.31 eV, $\Gamma_4^- = -10.62$ eV. The observed initial-state lifetime broadening (full width of half maximum) is 0.3 eV at the top of the d bands and 0.5 eV at the bottom of the d bands.

INTRODUCTION

Accurate valence-band energy dispersions $E(\vec{k})$ of a number of three-dimensional solids (Fe, Co, Ni, Cu, Pd) have been determined recently using angle-resolved photoemission-spectroscopy (ARPES) techniques combined with tunable synchrotron radiation (see, e.g., Refs. 1–4 and references therein). These $E(\vec{k})$ dispersions, which are of central importance in the single-particle description of solids, have given new information showing that the valence electrons of transition metals can be well described by an itinerant band model. Major discrepancies have been observed only for Ni, and for Co to a lesser extent, where d-band widths and magnetic exchange splittings are observed to be smaller than *ab initio* calculations predict (Ref. 4). The present ARPES investigation of Zn 3d states was undertaken in order to study the transition from itinerant bands to highly correlated, corelike levels. The investigation of this transition and the question of Ligand field splittings of outer core levels are of fundamental interest. Also of interest are the effects of final-state hole-lifetime broadenings when they are comparable to band-dispersion widths.

The question of $E(\vec{k})$ dispersion versus atomic-like behavior for deep-lying valence states, such as the Zn 3d states has never been studied thoroughly despite its fundamental importance. Generally, nondispersive atomiclike Zn 3d core levels have been assumed. Experimentally, the electronic structure of the Zn 3d states has not been determined accurately until now, despite several ultraviolet photoelectron spectroscopy (UPS),[5–7] soft x-ray emission,[8] and x-ray photoemission spectroscopy (XPS) (Refs. 9, 10) studies. XPS measurements are insensitive to small energy-band dispersions due to the energy resolution ($\Delta E \sim 0.5$ eV) and to the fact that they tend to sample bands throughout large regions of the Brillouin zone. However, band-structure calculations[11–15] show distinct 3-d band dispersions[12–15] with total d-band widths of the order of 1.4 eV (L_3 to L_1) (Refs. 13 and 15).

Concerning other materials with narrow bands, angle-integrated photoemission experiments for the valence bands of rare-gas solids with binding energies ranging from ~9.8 eV in Xe to ~20.3 eV in Ne (referred to the vacuum level) have given evidence of a bandlike behavior for the p-like deep-lying valence bands of these materials.[16,17] However, all available band-structure calculations to date have failed in predicting the bandwidths and hence the dispersions for these simple materials.

Using angle-resolved photoemission combined with polarized tunable synchrotron radiation, we have determined energy-band dispersions $E(\vec{k})$ for the 3d bands of Zn along the line Γ-A in $\vec{k}$ space. The upper d band shows a small (0.17 eV) but distinct dispersion which is indicative of itinerant band behavior. Also, we find matrix element and polarization-selection-rule effects for the Zn 3d states. Our findings are compatible with an itinerant band picture if the calculated 3d bands are empirically shifted to have the experimentally observed binding energies. Namely, a self-consistent *ab initio* calculation using the Hedin-Lundqvist local density approximation[18] yields Zn 3d bands centered at 8 eV below E_F with a 1.5-eV total bandwidth. This differs significantly from our findings, i.e., 3d bands centered at 10 eV below E_F with a 1.0-eV total bandwidth. However, upon correcting the d-band position via the use of an exchange parameter $\alpha = 0.8$ in a nonrelativistic $X\alpha$ calculation, the calculated total bandwidth becomes 1.0 eV and the upper d-band-dispersion width becomes 0.25 eV, in reasonable agreement with experiment. Even bet-

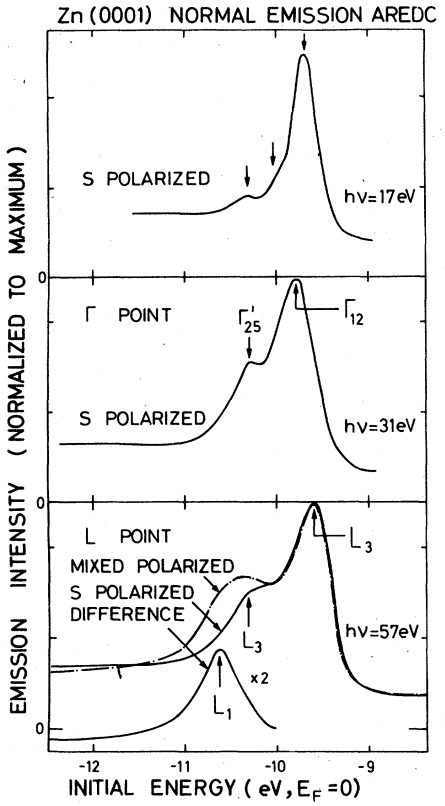

FIG. 1. Angle-resolved photoelectron spectra from Zn (0001) for a selected set of photon energies showing the photon and polarization dependence of the $3d$ emission in the [0001] direction. Solid lines give the s-polarized spectra whereas the dash-dotted line in the lower panel shows the result for mixed polarized geometry. The difference curve in the lower panel empahsizes the contribution from the L_1 point (see text).

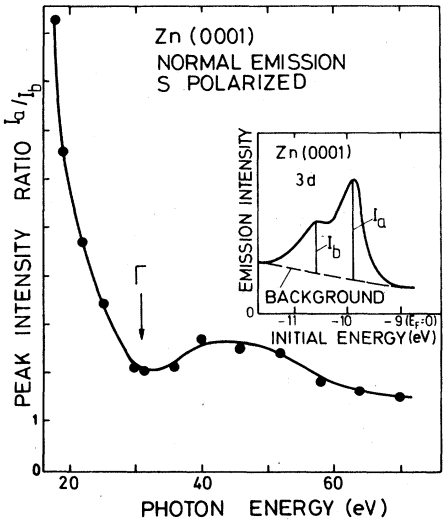

FIG. 2. Photon-energy-dependent intensity ratio I_a/I_b of the $3d$ "doublet" lines in s polarization. The local minimum at 31 eV photon energy occurs at the Γ point in k space.

ter agreement is obtained when the hcp lattice is taken into account.

EXPERIMENTAL TECHNIQUES

For our measurements, a two-dimensional display-type electron spectrometer was used.[19] Synchrotron radiation from the 240-MeV storage ring Tantalus I at the University of Wisconsin in Madison monochromatized by a 1.5-m toroidal grating

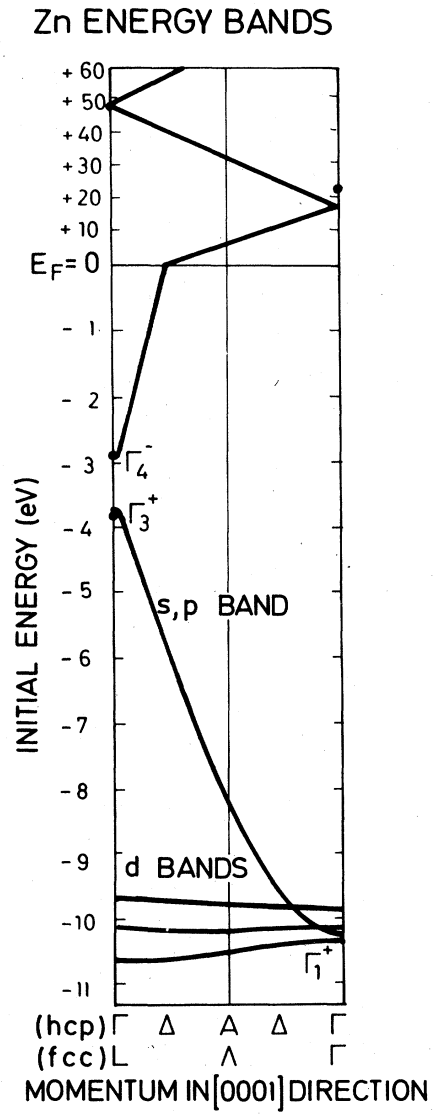

FIG. 3. Schematic energy-band dispersion E vs $\vec{k}$ for Zn. Note the change in the energy scale (by a factor of 20) at the Fermi level E_F. The valence bands are from Juras *et al* (Ref. 13, $\alpha=1$), and the bands above E_F are free-electron-like bands (bottom at 8 eV below E_F) with experimental critical points marked by dots. Two sets of symmetry labels (for fcc and hcp lattices) are given (for details of comparing fcc and hcp Brillouin zones, see Ref. 3).

monochromator served as a tunable light source. The combined energy resolution of the monochromator and electron spectrometer was ≤ 200 meV for the photon-energy range $5 \leq h\nu \leq 60$ eV used in this study. The electron spectrometer was operated at an angular resolution of $\delta\Theta = 6°$. For these conditions, typical counting rates ranged from 10^3/sec to 10^5/sec for the Zn $3d$ bands. Normal emission spectra were taken from a Zn (0001) face prepared by sputter etching and annealing and characterized by low-energy electron diffraction (LEED) and Auger electron spectroscopy. Two different light polarizations were used: s polarization with $E \parallel [10\bar{1}0]$ and mixed s,p polarization. For Zn (0001) we have determined a work function of $e\Phi = 4.4$ eV.

EXPERIMENTAL RESULTS AND DISCUSSIONS

Angle-resolved photoelectron spectra of the Zn $3d$ bands are shown in Fig. 1 for several selected photon energies and polarizations. The most intense emission comes from the uppermost d band, with weaker emission from lower lying d bands. As we will discuss, interband transitions at Γ occur for $h\nu = 31$ eV and transitions at L (fcc notation) occur for $h\nu = 57$ eV. Thus, the energy dispersion of the upper d band is given by the energy difference (0.17 eV) of the L_3 ($h\nu = 57$ eV) and Γ_{12} ($h\nu = 31$ eV) critical-point energies. Further, the spectra show a polarization dependence; namely, for $h\nu = 57$ eV an extra transition which is forbidden in s polarization is seen for mixed s-p polarization (i.e., the L_1 transition, see difference spectrum). All of these observations are not compatible with an atomic core-level model [the $3d$ spin-orbit splitting is 0.34 eV (Ref. 20) in atomic Zn].

The Zn $3d$ states show itinerant band behavior analogous to d states for other transition and noble metals (Fe, Co, Ni, Cu, Pd) and we shall next describe our experimentally determined $E(\vec{k})$ dispersions for Zn and compare them with band calculations. We shall use fcc lattice-symmetry labels as well as hcp symmetry labels by taking advantage of a relationship between these crystal lattices which is valid for normal emission along the hcp [0001] axis (Ref. 3).

In Fig. 2 the photon-energy-dependent intensity ratio of the $3d$ doublet lines for s polarization is shown. The lower d-band peak (b) becomes very weak for low photon energies and has a relative maximum at $h\nu \sim 31$ eV. Qualitatively, the same behavior is seen for other fcc or hcp transition metals[1-3] and the minimum of the intensity ratio I_a/I_b corresponds to interband transitions at the center of the Brillouin zone Γ. This yields an energy of ~21 eV above E_F for the final state at Γ. With increasing $h\nu$, one moves along the line ΓL

TABLE I. Experimental and calculated critical points for the $3d$ bands of Zn (energies in eV with $E_F = 0$). The fcc-symmetry labels are correlated to hcp-symmetry labels according to Ref. 3.

Symmetry point fcc	Symmetry point hcp	This experiment	Juras *et al.*[a]	Juras *et al.*[b]	Moruzzi *et al.*[c]
L		$+47 \pm 2$[d]			
Γ		$+21 \pm 2$			
L_1	Γ_4^-	-2.9 ± 0.3[d]	−2.9	−2.7	−1.20
L_2'	Γ_3^+	-3.9 ± 0.3[d]	−3.7	−4.0	−3.33
L_3	Γ_5^-	-9.60 ± 0.03	−9.7	−7.3	−7.48
Γ_{12}	Γ_6^+	-9.77 ± 0.03	−9.9	−7.6	−7.81
Γ_{25}'	Γ_6^-	-10.05 ± 0.1[e] -10.30 ± 0.05[e]	−10.15	−8.0	−8.21
L_3	Γ_5^+	-10.05 ± 0.1[e] -10.31 ± 0.05[e]	−10.1	−7.9	−8.24
L_1	Γ_4^-	-10.62 ± 0.05	−10.6	−8.9	−8.99

[a] Reference 13, $X\alpha$ calculation ($\alpha = 1$), hcp lattice.
[b] Reference 13, $X\alpha$ calculation ($\alpha = \frac{5}{6}$), hcp lattice.
[c] Reference 15, self-consistent calculation using Hedin-Lunqvist exchange, fcc lattice.
[d] Discussed in more detail in Ref. 21.
[e] The experimental splitting is probably due to spin-orbit effects which are not included in the calculations. All symmetry labels are nonrelativistic.

(fcc lattice) or $\Gamma A \Gamma$ (hcp lattice) in $\vec{k}$ space (see Fig. 3). The final-state L point is located at ~47 eV above E_F by following the dispersion of the s-p band (see Fig. 3 and Ref. 21). The $3d$ states are excited into this final state at $h\nu \sim 57$ eV. Critical-point energies at Γ and L for initial states (e.g., Fig. 1) and final states are summarized in Table I.

The overall shift of spectral weight from the upper part of the d bands to the lower part of the d bands with increasing photon energy may explain previous discrepancies between UPS data ($h\nu = 21.2, 40.8$ eV) and XPS data ($h\nu = 1487$ eV) where the doublet structure of the Zn d-band emission was not resolved. The values for the d-band position reported by UPS [-9.5 eV,[5,6] -9.9 eV (Ref. 7)] were consistently higher than XPS values [-10.18 eV,[6] -10.08 eV (Ref. 10)].

Energy-band dispersions $E(\vec{k})$ for the Zn $3d$ bands have been determined from a set of normal-emission energy-distribution curves for $15 \leq h\nu \leq 70$ eV (along the c axis, not shown). These experimental $E(\vec{k})$ dispersions are summarized in Fig. 4. To determine the momentum scale along the ΓL (i.e., $\Gamma A \Gamma$) direction, we have converted the measured final energy to the momentum $\vec{k}$ via a final-state nearly-free-electron energy-band dispersion (see Fig. 3). This nearly-free-electron (nfe) parabolic final band ($m^* = m_e$), with a potential zero at 8 eV below E_F (Ref. 15) approximates our experimentally determined final-state critical points as well as Fermi-surface data[11] (see Fig. 3). The E-$\vec{k}$ conversion scale for the nfe final band is shown on top of Fig. 4, e.g., a final energy of $E = 47$ eV corresponds to interband transitions near L. As shown for Co (0001) in Ref. 3, the bands along $\Gamma A \Gamma$ in an hcp lattice can be unfolded to correspond to the line ΓL of an fcc lattice. Accordingly, two sets of labels for the symmetry points are given on the bottom of Fig. 3 and Fig. 4. The upper d band with Λ_3 symmetry disperses 0.17 eV upward from Γ to L, the lower d band with Λ_3 symmetry has no measurable dispersion. Qualitatively, this is very similar to the d-band dispersion seen for Cu, Ni, Pd, etc. The lower Λ_3 band seems to be split (~0.25 eV) by spin-orbit effects.

In Tables I and II experimental critical-point energies at Γ and L and band dispersions for Zn are summarized and compared with a self-consistent *ab initio* energy-band calculation[15] which used a local density approximation (i.e., Hedin-Lundqvist potential), as well as with an earlier non-self-consistent calculation[13] which used exchange coefficients $\alpha = \frac{5}{6}$ and $\alpha = 1$. Labels are given for non-relativistic bands in an fcc and hcp lattice. There is a one-to-one correspondence except for the Γ_{25}' point, which is split into the Γ_1^+ and Γ_6^- points in the hcp lattice. There is a systematic discrepancy between the experimental and *ab initio* calculated bands; the calculated bands are too wide and their center of gravity is too high by ~2 eV. This comparison shows more dramatically a trend which was observed in Cu (Ref. 2) and attributed to inadequate self-energy corrections. We note that the above comparison involves experimental excited-state eigenvalues versus calculated ground-state single-particle energies; such comparisons always involve questions concerning relaxation effects which ac-

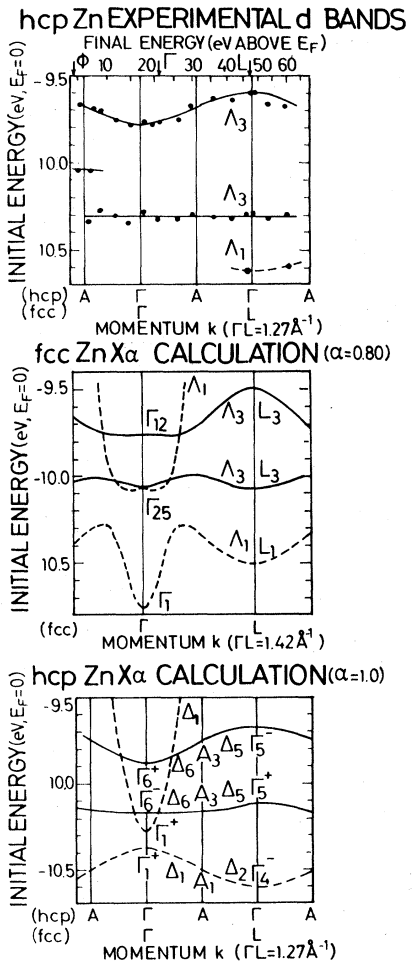

FIG. 4. Experimental and calculated Zn $3d$-band disperions. The experimental data are in the uppermost panel. The $E(k_\perp)$ conversion scale for the free-electron like final band energy is given on top; e.g., a final energy of 47 eV corresponds to a momentum $\vec{k}$ near the L point (Γ in hcp notation, see text). Directly determined critical points are marked by arrows. The middle panel shows the result of a self-consistent $X\alpha$ ($\alpha = 0.80$) calculation which was performed for an fcc lattice. The bottom panel shows the result of an $X\alpha$ ($\alpha = 1$) calculation by Juras *et al.* (Ref. 13). Dashed bands are forbidden in normal emission with s polarization (i.e., Λ_1 symmetry and Δ_1, Δ_2 symmetry for an fcc and hcp lattice, respectively).

TABLE II. Experimental and calculated band parameters for the 3*d* bands of Zn (energies are in eV).

	This experiment	Juras *et al.*[a]	This calculation[b]	Juras *et al.*[c]	Moruzzi *et al.*[d]
$\Gamma_6^+ - E_F$ (3*d*-band position)	−9.77 ± 0.03	−9.9	−9.76	−7.6	−7.81
$\Gamma_5^- - \Gamma_4^-$ (3*d*-band full width)	1.02 ± 0.05	0.9	1.01	1.55	1.51
$\Gamma_5^- - \Gamma_6^+$ (3*d*-band dispersion)	0.17 ± 0.05	0.19	0.25	0.30	0.33

[a] $X\alpha$ calculation ($\alpha = 1.0$), hcp lattice, Ref. 13.
[b] Self-consistent $X\alpha$ calculation ($\alpha = 0.80$), fcc lattice.
[c] $X\alpha$ calculation ($\alpha = \frac{5}{6}$), hcp lattice, Ref. 13.
[d] Self-consistent calculation with Hedin-Lundqvist exchange, fcc lattice, Ref. 15.

company electronic excitations.

We have performed a self-consistent field (SCF) $X\alpha$ calculation which "matches" the experimental 3*d*-band position by selecting an exchange parameter of $\alpha = 0.8$. These calculated bands are shown in Fig. 4. Upon being lowered by ~2 eV to the experimental *d*-band position, the *d* bands become narrower (e.g., see Connolly[22]) and band dispersions become smaller. This narrowing results in a good agreement with experiment (e.g., L_3-L_1 separations in Table II). The band dispersion of the upper *d* band is still too large in this calculation; this could be due to the fact that relativistic effects have been neglected and also that an fcc lattice rather than hcp lattice has been used. Spin-orbit effects, which cause a 0.34-eV splitting for the free atom, must be included in more realistic calculations. To estimate the effect of an hcp versus fcc lattice, we have taken a non-self-consistent $X\alpha$ calculation for an hcp lattice (Ref. 13, $\alpha = 1$) and find almost perfect agreement with our experiment (Table II, Fig. 4).

Our experimental data can also be used to obtain hole lifetimes τ from the width of the observed peaks in angle-resolved photoelectron spectra at critical points. We find an inverse lifetime ($\Gamma = \hbar/\tau$) of $\Gamma \leq 0.3$ eV at the top of the *d* bands and $\Gamma = 0.5$ eV at the bottom of the *d* bands (L_1, Γ_4^-, respectively). These values represent upper bounds on the intrinsic lifetimes; experimental broadening contributions due to the monochromator and electron spectrometer are small.

We believe that the Zn *d* bands are an ideal test case for self-energy effects which go beyond the local density approximation. We have measured the imaginary part of the self-energy (the inverse lifetime) as well as the real part of the self-energy which determines the band position. It would be interesting to apply self-energy corrections to an *ab initio* calculation for the Zn 3*d* bands. Similar efforts have been started for nickel[23-26] and copper[27] where the self-energy effects are less dramatic than in zinc.

*IBM summer visitor, permanent address: Hamburger Synchrotronstrahlungslabor, HASYLAB, Deutsches Elektronen-Synchrotron DESY, Hamburg, Federal Republic of Germany.

[1] F. J. Himpsel and D. E. Eastman, Phys. Rev. B 18, 5236 (1978).
[2] J. A. Knapp, F. J. Himpsel, and D. E. Eastman, Phys. Rev. B 19, 4952 (1979).
[3] F. J. Himpsel and D. E. Eastman, Phys. Rev. B 21, 3207 (1980).
[4] D. E. Eastman, F. J. Himpsel, and J. A. Knapp, Phys. Rev. Lett. 44, 95 (1980).
[5] P. O. Nilsson and I. Lindau, J. Phys. F 1, 854 (1971).
[6] P. T. Poole, R. C. G. Leckey, J. G. Jenkin, and J. Liesegang, Phys. Rev. B 8, 1401 (1973).
[7] I. Abbati, L. Braicovich, G. Giucci, and P. Perfetti, J. Vac. Sci. Technol. 16, 863 (1979) and references therein.
[8] R. J. Liefeld, in *Soft X-ray Band Spectra and the Electronic Structure of Metals and Materials*, edited by D. Fabian (Academic, New York, 1968).
[9] L. Ley, S. P. Kowalczyk, F. R. McFeely, R. A. Pollak, and D. A. Shirley, Phys. Rev. B 8, 2392 (1973).
[10] Previous XPS studies have suggested that 3*d*-band broadening is significant; S. K. Wertheim, M. Campagna, and S. Hüfner, Phys. Condens. Matter 18, 133 (1974).
[11] R. W. Stark and L. M. Falicov, Phys. Rev. Lett. 19, 795 (1967).
[12] F. Borghese and P. Denti, Nuovo Cimento 3B, 34 (1971).
[13] G. E. Juras, B. Segall, and C. B. Sommers, Solid State Commun. 10, 427 (1972); unpublished results of this calculation have been communicated to us privately

by B. Segall.
[14]F. J. Arlinghaus, Phys. Rev. 186, 609 (1969).
[15]V. L. Moruzzi, A. R. Williams, and J. F. Janak, *Calculated Electronic Properties of Metals* (Pergamon, New York, 1978).
[16]N. Schwentner, F. J. Himpsel, V. Saile, M. Skibowski, W. Steinmann, and E. E. Koch, Phys. Rev. Lett. 34, 528 (1975).
[17]A. B. Kunz, D. J. Mickish, S. K. V. Mirmira, T. Shima, F. J. Himpsel, V. Saile, N. Schwentner, and E. E. Koch, Solid State Commun. 17, 761 (1975).
[18]L. Hedin and B. I. Lundqvist, J. Phys. C 4, 2064 (1971).
[19]D. E. Eastman, J. J. Donelon, N. C. Hien, and F. J. Himpsel, Nucl. Instrum. Methods 172, 327 (1980).
[20]C. E. Moore, *Atomic Energy Levels*, U. S. National Bureau of Standards, Circular No. 467 (U.S. GPO, Washington, D. C., 1958).
[21]F. J. Himpsel, E. E. Koch, and D. E. Eastman (unpublished).
[22]J. W. D. Connolly, Phys. Rev. 159, 415 (1967).
[23]A. Liebsch, Phys. Rev. Lett. 43, 1431 (1979).
[24]L. C. Davis and L. A. Feldkamp, Solid State Commun. 34, 141 (1980).
[25]D. Penn, Phys. Rev. Lett. 42, 921 (1979).
[26]G. Treglia, F. Ducastelle, and D. Spanjaard, Phys. Rev. B 21, 3729 (1980).
[27]F. Sachetti (unpublished).